Journal of Mining and Earth Sciences

Website: http://jmes.humg.edu.vn

Improving carbonate reservoir characterization by applying rock typing methods: a case study from the Nam Con Son Basin, offshore Vietnam

Man Quang Ha [1*], Hoa Minh Nguyen [2], Dung Viet Bui [3], Hong Viet Nguyen [4], Hoa Khac Truong [1], Ngoc Quy Pham [3],

[1] *PetroVietnam Exploration Production Corporation, Hanoi, Vietnam*
[2] *Hanoi University of Mining and Geology, Hanoi, Vietnam*
[3] *Vietnam Petroleum Institute, Hanoi, Vietnam*
[4] *Schlumberger Vietnam, HoChiMinh City, Vietnam*

ARTICLE INFO

Article history:
Received 26th July 2022
Revised 07th Nov. 2022
Accepted 15th Dec. 2022

Keywords:
Carbonate,
Miocene,
Nam Con Son basin,
Permeability,
Rock type.

ABSTRACT

Understanding the permeability-porosity relationships is the key to improving reservoir prediction and exploitation especially in carbonate reservoirs, which are known for their complex textural and diagenetic variation. Rock type classifications have long been proven to be an effective technique for establishing permeability- porosity relationships, enhance the capability to capture the various reservoir flow behavior and prediction for uncored reservoir zones. This study highlights some of those practical and theoretically-correct methods, such as Hydraulic Flow Unit (HFU); Global hydraulic element (GHE), Winland's R_{35} method, Pittman method, Lucia method. They are proposed and tested for identification and characterization of the rock types using a database of 555 core plugs from the Miocene carbonate reservoir in the Nam Con Son basin. It is a large isolated carbonate build-up structure which were deposited within a shallow marine platform interior and are dominated by coral, red algal and foraminiferal packstones, wackestones and grainstones. Hydrocarbons in this reservoir have been found in the upper most part of the late Miocene formation. Conventional core data were first used to define and display the cross plot of permeability and porosity. Different charts and cutoff thresholds were used to classified, defined number of rock type and the linear and non-linear equations were established. The predicted core permeability was calculated using different methods and compared with the actual core permeability for each rock type. The predicted reservoir rock type and permeability predictions of HFU method was recognized to give better matching of measured core permeability with coefficient of more than 89%.

*Corresponding author
E - mail: manhq@pvep.com.vn
DOI: 10.46326/JMES.2023.64(1).05

1. Introduction

A significant proportion of the world's oil reserves is found in carbonate reservoirs. Carbonate reservoir evaluation is challenging because of the presence of complex pore size distribution with widely varying proportions of primary and secondary porosity. This has a significant impact on the fluid flow characteristics and hence the permeability of the reservoir.

Rock-typing is an effective technique for investigating porosity-permeability relationships and predicting the permeability from well log-derived porosity in un-cored wells. This has enabled accurate generation of initial water saturation profiles and, consequently, reliable reservoir simulation studies (Guo et al., 2007; Shenawi et al., 2007).

Several rock typing approaches have been developed such as: Flow zone indicator - FZI (Amaefule et al., 1993); Global hydraulic element - GHE (Corbett et al., 2003); Winland's R_{35}; Pittman (Pittman, 1992) and Lucia (Lucia, 2007).

The objective of this study is to review and compare the best-known clustering methods of rock-typing, and to deliver the most appropriate approach for carbonate facies classification and its porosity-permeability transform.

2. Geological setting of the Nam Con Son Basin

The Nam Con Son basin (NCSB) is located in the southeastern continental shelf of Vietnam. The basin is bordered with the Cuu Long basin in the west, the Tu Chinh - Vung May basin in the East and the Phu Khanh basin in the North east (Figure 1). Although there were likely tectonic influences affecting this area in the pre-Tertiary (Matthews et al., 1997), the first rifting event forming the NCSB occurred in the late Eocene to early Oligocene. This was associated with the onset of north - south opening of the east Vietnam sea. From seismic evidence, there appears to be a stratigraphic interval that could be interpreted as Eocene to Early Oligocene. This interval terminates upwards in a major breakup unconformity at the top of Early Oligocene. This early rifting was followed by thermal sag associated with the post-rift phase. During the Early Miocene, south west (SW) propagation of east Vietnam sea floor spreading to the north east (NE) of the basin and other regional tectonic forces impacted the NCSB. This eventually lead to a second rifting phase followed by a regional uplift event in late Middle Miocene as evidenced by the Mid-Miocene Unconformity (MMU). The post rift section during late Miocene to present is marked

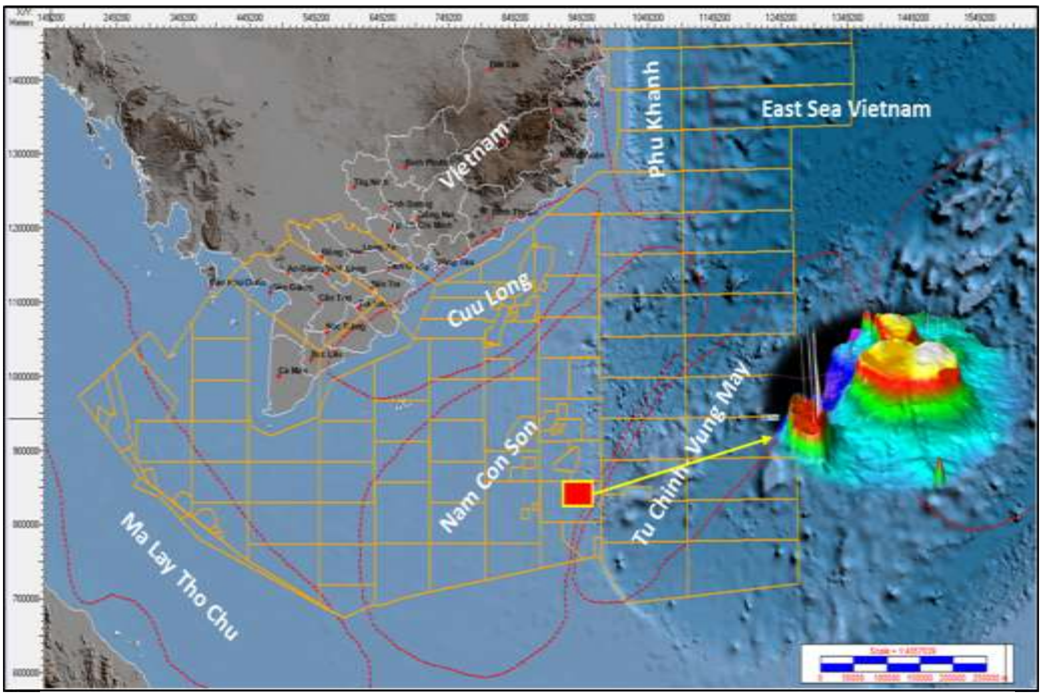

Figure 1. Overview of carbonate distribution in the study area (red rectangle).

by thermal sag and the progradation of the Paleo-Mekong Delta into the basin. Miocene carbonate reservoirs, including both platform and reef, are mainly distributed in the East of the NCSB. Carbonate deposition was initiated on the structural highs during late Early Miocene; widely developed during the Middle and late Miocene; and mostly terminated in early Pliocene (Bui et al., 2018).

The study area lies in the SE of the NCSB, offshore in a water depth of about 125 meters (Figure 1). The reservoir is a large isolated carbonate build-up structure with an average thickness of 500m covering an area of about 50 km^2. The build-up comprises Late Miocene carbonates overlaying a more extensive Middle Miocene carbonate platform. The carbonates were deposited within a shallow marine platform interior and are dominated by coral, red algal and foraminiferal packstones, wackestones and grainstones. Hydrocarbons in this reservoir have been found in the upper most part of the late Miocene formation.

3. Methodology and data

In this study, the core plug data from the Miocene carbonate reservoir in the NCSB were classified according to rock type. Six rock typing classification methods were applied. To select the best rock typing method, the results were calculated the correlation coefficient (R^2) between predicted permeability (K_pre) and core permeability (K_core) for each rock typing method. Figure 2 shows a workflow for this study.

3.1. Hydraulic flow unit (HFU)

This method includes reservoir quality index (RQI) and Flow zone analysis. RQI reflects the reservoir properties and flow unit indicators can be inferred by the RQI, which reflects permeability of different rock types and regardless of the depositional facies of the formation. Amaefule et al (1993) introduced two auxiliary factors: Φz, the normalized porosity - Equation (1); and RQI - Equation (2). This results in a new formula - Equation (3), which defines Flow zone indicator (FZI) in terms of porosity-permeability relationships, which accurately approximate the reservoir quality for a given sedimentary facies (Amaefule et al., 1993; Svirsky et al., 2004; Guo et al., 2007; Shenawi et al., 2009; Abdallah et al., 2016; Ha et al., 2021 a,b).

$$\Phi_z = \frac{\Phi_e}{1 - \Phi_e} \tag{1}$$

$$RQI = 0.0314\sqrt{\frac{K}{\Phi_e}} \tag{2}$$

$$FZI = \frac{RQI}{\Phi_z} = 0.0314\left(\frac{1-\Phi_e}{\Phi_e}\right)\sqrt{\frac{K}{\Phi_e}} \tag{3}$$

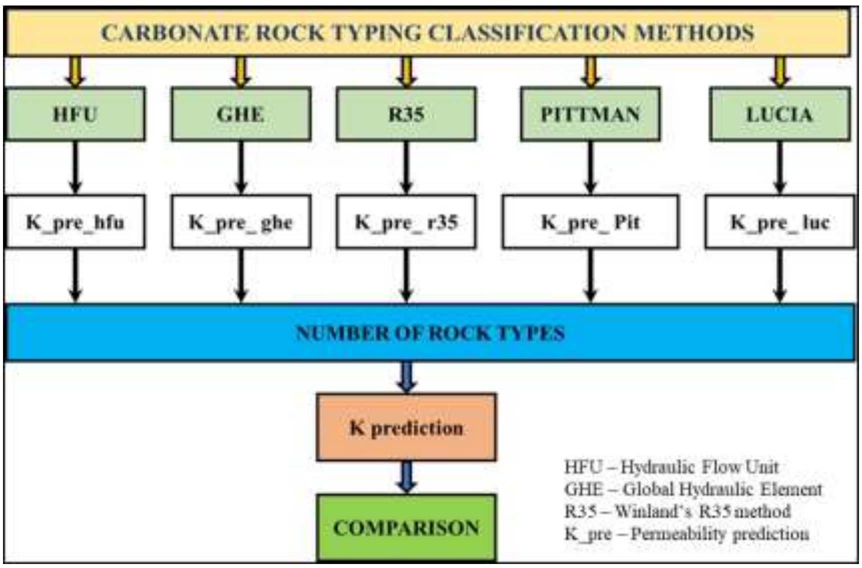

Figure 2. The workflow of this study for rock typing in carbonate reservoirs.

Where: Φ_e - the effective porosity (v/v), K - permeability (mD), RQI - µm and FZI - µm.

3.2. Global hydraulic element (GHE)

Global hydraulic element method was developed by Peter Corbett et al (2003). They suggested using GHE based on a priori systematic series of FZI values with the purpose of splitting a wide range of possible combinations of porosity and permeability into a manageable number of GHE. They constructed a GHE template on the porosity versus permeability crossplot and split the parameter space into 10 GHE. The advantages of this approach are that there is no need to do cluster analysis on the core data from any reservoir, which is compared on exactly the same reference frame. This approach is gaining popularity compared to the conventional hydraulic unit approach described by Amaefule et al. (1993). The permeability can be calculated by a rearrangement of equation (3):

$$K = \Phi_e \left[\frac{FZI.\frac{\Phi_e}{1-\Phi_e}}{0.0314} \right]^2 \qquad (4)$$

As a result, this method determines FZI values for each kind of GHE shows on Table 1 below:

Table 1. FZI mean value for each GHE by Corbett et al. (2003).

GHE	FZI	GHE	FZI
10	48	5	1.5
9	24	4	0.75
8	12	3	0.375
7	6	2	0.1875
6	3	1	0.0938

3.3. Winland's R_{35} method

During the 1970s Winland developed a method that focused on the relationship between porosity, permeability and pore throat radius. He applied this to reservoir rocks of both clastic and carbonate reservoirs from Spindle field. He tested 312 water-wet samples to evaluate sealing potential. Winland proved his method with the results from Mercury Injection Capillary Pressure (MICP) testing such as porosity, permeability and 30%, 35%, 40% and 50% radius frequency of effective porosity. His experiments revealed that the effective pore system that dominates flow through rocks in his set of samples corresponded to a mercury saturation of 35%. Winland's tabulated the correlation between porosity, permeability and pore throat size using sandstones and carbonate samples as follow:

$$Log\ R_{35} = 0.732 + 0.588\ log\ K - 0.864\ log\ \Phi \qquad (5)$$

Where: Φ - porosity (%), K - the uncorrected air permeability (mD), and R_{35} - the pore throat radius at 35% mercury saturation form MICP test. Many researchers have applied this method to improve reservoir characterization such as Kolodzie (1980); Harmann and Beaumont (1999); Pitman, (1992); Spearing et al. (2001); Palabiran et al. (2016); Haikel et al. (2018).

3.4. Pittman method

Pittman (1992) extended the Winland's method based on capillary pressure measurement from 196 sandstone samples to find out greater accuracy the modal class of pore throat size. Pittman improved the Winland's method and developed an equation to calculate pore aperture radii corresponding to mercury saturation values that range from 10÷75% in increments of 5%. The Pittman equation for pore throat size at 35% non-wetting phase saturation as follow:

$$Log\ R_{35} = 0.255 + 0.565\ log\ K - 0.523\ log\ \Phi \qquad (6)$$

Where: Φ - porosity (%), K - the uncorrected air permeability (mD), and R_{35} - the pore throat radius at 35% mercury saturation frequency form MICP test.

3.5. Lucia method

The Lucia method is an attempt at a universal classification petrophysical properties in carbonate reservoirs, based on interparticle porosity (Rebelle and Lalanne, 2014). Lucia defined three main carbonate rock classes defined by their Rock Fabric Number (RFN) below:

- Class 1: grain dominated Fabric - Grainstone. RFN's of 0.5÷1.5.
- Class 2: grain dominated Fabrics - Packstone. RFN's of 1.5÷2.5.

- Class 3: Mud-dominated Fabrics - Packstone, Wackestone, Mudstone. RFN's of 2.5÷4.0.

The Rock Fabric number is calculated from:

$$RFN = A.\,log\frac{9.7982 + 8.6711\,log(\Phi) - log(K)}{12.0838 + 8.2965\,log\,(\Phi)} \quad (7)$$

Where: porosity Φ - in decimals and permeability K - in milli-darcies.

When total porosity is derived from logs, the core-log depth match has to be very accurate to be associated with a given thin section. Moreover, porosity acquisition scale from logs and plugs are largely different and large discrepancies could be observed between both (Palabiran et al., 2016; Haikel et al., 2018).

3.6. Data set

In this study, some core data comprised porosity and permeability and short lithology description. We used 555 cores data samples (K_core and Phi_core) from 3 wells. Histograms of porosity (a), permeability (b) and FZI (c) and a cross plot (d) of permeability vs. porosity are presented in Figure 3.

4. Results and discussions

In the study, rock type classification for carbonate reservoir has tested for 555 cores plug data from routine core analysis using the five methods which have been described above. The results of each method will be summarized and discussed below.

4.1. GHE method

In order to overview and recognize all of the rock types in this carbonate reservoir, the first method we applied was the GHE method. In this method, FZI was calculated from core porosity and permeability and used as a key parameter to classify reservoir into different GHE. In the next step, the core porosity (PHI_core) and permeability (K_core) data was projected onto the appropriate GHE template constructed for each GHE. As a result, 8 distinct GHE (range from GHE_2 to GHE_10) were defined on the basis 555 available core samples (Figure 4a). Within each GHE, permeability is predictable on the basis of a strong porosity-permeability relationship given by equation 4. The crossplot of measured permeability versus permeability calculated for

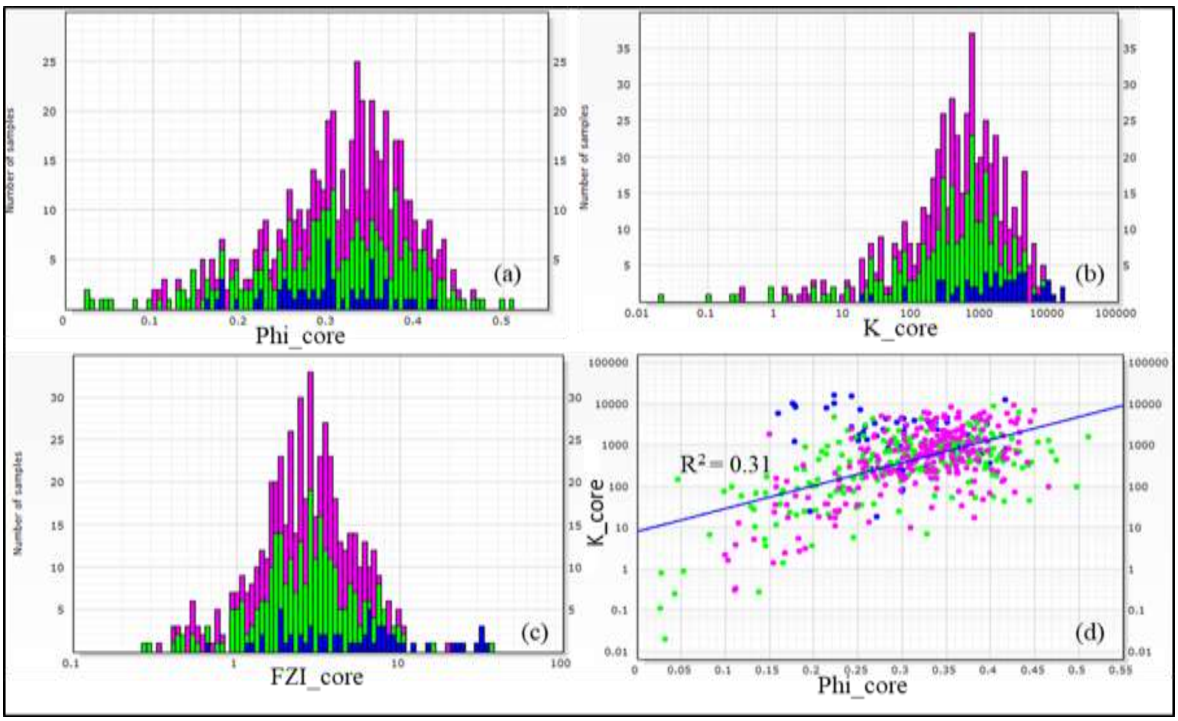

Figure 3. The core data from 3 wells are using in this study: histogram of porosity (a), permeability (b), FZI (c) and cross plot of permeability versus porosity for 555 cores data (d).

groups of various FZI mean (Table 1) is shown in Figure 4b, where the correlation coefficient of $R^2 = 0.95$ is nearly perfect.

4.2. HFU method

The second method for carbonate rock typing classification is based on the HFU method. In this part, we can define each rock type is equal to an HFU. In this method, HFU classification based on the histogram (Figure 5a), the probability plot and Ward's clustering method suggested a division of data into FZI groups. To compare the results with GHE method above, we also try to divide the carbonate reservoir into eight clusters that corresponding to eight HFU or eight rock types.

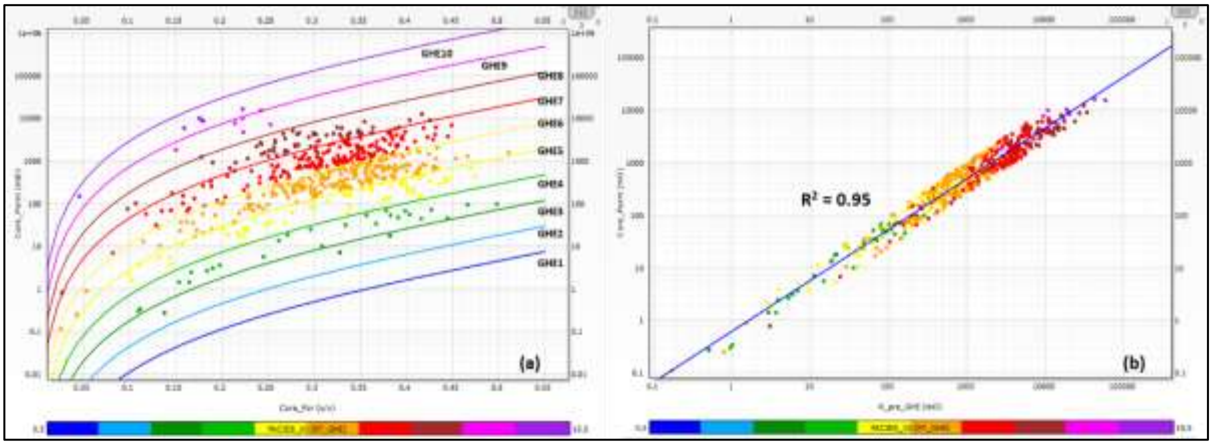

Figure 4. The results of GHE method: (a) crossplot permeability vs. porosity data on the background of 8 GHE; (b) crossplot of K_ghe that calculated on the basis of relationship FZI and PHI_core for 8 GHE versus K_core.

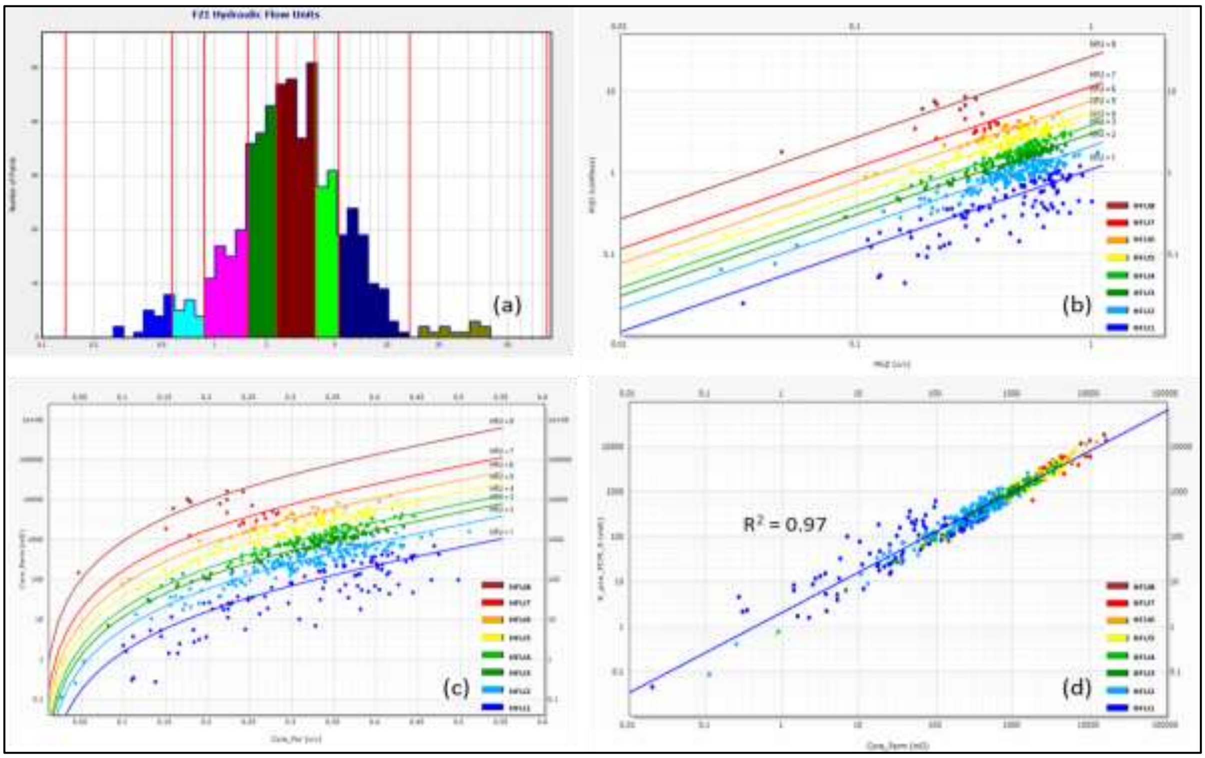

Figure 5. The results of HFU method: (a) FZI histogram; (b) the crossplot PHIz versus RQI; (c) the crossplot Phi_core and K_core color corresponding with 8 HFU; (d) the crossplot to compare K_core and K_pre for HFU method.

On the basis of HFU classification, a plot of PHIz versus RQI for each HFU was constructed (Figure 5b). Analysis of the crossplot PHIz versus RQI showed a distinct grouping into 8 HFU classes (Figure 5c) according to mean FZI values (Table 2). The permeability can be predicted for each HFU using the 8 equations from 8a to 8k. The crossplot of measured permeability (K_core) versus calculated permeability (K_hfu) for groups of various FZI mean (Table 2) reveals a nearly perfect correlation (R^2 = 0.97) (Figure 5c).

4.3. Winland's R35 method

Based on radius of effective pore, the distribution of porosity and permeability core at isopore throat line as can see on Figure 6a and from this plot we can get rock type based on similarity of effective pore size by Winland's R_{35} method. In order to compare the results with HFU method above, we also try to divide carbonate reservoir into 8 RT_R_{35} classes. Table 3 summarizes the statistics of each RT_ R_{35}. The permeability was calculated (K_pre_ R_{35}) for this

Table 2. Simple statistics of parameters for 8 RT_hfu.

RT_hfu	Name	Start	Stop	Mean	Values	R^2
1	RT_hfu 1	0.137	0.571	0.45	20	0.9573
2	RT_hfu 2	0.571	0.876	0.70	16	0.9885
3	RT_hfu 3	0.876	1.581	1.234	71	0.9517
4	RT_hfu 4	1.581	2.319	1.921	112	0.9692
5	RT_hfu 5	2.319	3.858	3.002	173	0.9367
6	RT_hfu 6	3.858	5.300	4.496	69	0.9665
7	RT_hfu 7	5.300	13.623	7.097	82	0.9079
8	RT_hfu 8	13.623	85.779	25.343	12	0.7822

RT_hfu1: $$K_1 = \Phi^3\left(\frac{0.450}{0.314\,(1-\Phi)}\right)^2 \quad 8a)$$

RT_hfu5: $$K_1 = \Phi^3\left(\frac{0.450}{0.314\,(1-\Phi)}\right)^2 \quad (8e)$$

RT_hfu2: $$K_2 = \Phi^3\left(\frac{0.7}{0.314\,(1-\Phi)}\right)^2 \quad (8b)$$

RT_hfu6: $$K_2 = \Phi^3\left(\frac{0.7}{0.314\,(1-\Phi)}\right)^2 \quad (8f)$$

RT_hfu3: $$K_3 = \Phi^3\left(\frac{1.234}{0.314\,(1-\Phi)}\right)^2 \quad (8c)$$

RT_hfu7: $$K_3 = \Phi^3\left(\frac{1.234}{0.314\,(1-\Phi)}\right)^2 \quad (8g)$$

RT_hfu4: $$K_4 = \Phi^3\left(\frac{1.921}{0.314\,(1-\Phi)}\right)^2 \quad (8d)$$

RT_hfu8: $$K_4 = \Phi^3\left(\frac{1.921}{0.314\,(1-\Phi)}\right)^2 \quad (8h)$$

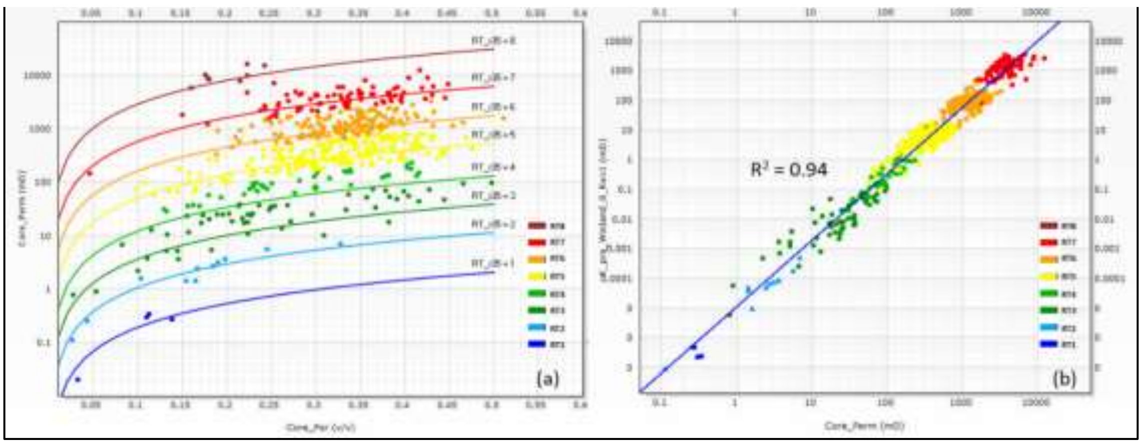

Figure 6. The results of Winland's R_{35} method: (a) cross plot permeability vs. porosity data on the background of 8 RT_ R_{35}; (b) cross plot K_ R_{35} calculated on the basis of relationship for 8 RT_ R_{35} versus K_core.

method using equations 9a÷9h. The crossplot of K_pre_ R_{35} versus K_core is shown in Figure 6b, where the correlation coefficient of R^2 = 0.94 is near perfect.

4.4. Pittman method

The Pittman method was developed from the Winland R_{35} method. Therefore, the step for rock type classification is similar. In order to compare the results with other methods above, we also try to divide carbonate reservoirs into 8 RT_pit classes. Figure 7a shows the results and Table 4

Table 3. Simple statistics for 8 RT_ R_{35}.

RT_r35	Name	Start	Stop	Mean	Values	R^2
1	RT_ R_{35} 1	0.11	0.456	0.279	4	0.88
2	RT_ R_{35} 2	0.456	1.005	0.762	11	0.95
3	RT_ R_{35} 3	1.005	3.335	2.155	54	0.76
4	RT_ R_{35} 4	3.335	5.432	4.427	40	0.85
5	RT_ R_{35} 5	5.432	11.857	8.336	202	0.57
6	RT_ R_{35} 6	11.857	25.047	16.735	155	0.32
7	RT_ R_{35} 7	25.047	66.715	33.147	81	0.62
8	RT_ R_{35} 8	66.715	163.595	90.804	8	0.54

RT_ R_{35}_1
$$K_1 = 10^{\frac{\log 0.279 - 0.732 + 0.864 \log \Phi}{0.588}} \quad (9a)$$

RT_ R_{35}_2
$$K_2 = 10^{\frac{\log 0.762 - 0.732 + 0.864 \log \Phi}{0.588}} \quad (9b)$$

RT_ R_{35}_3
$$K_3 = 10^{\frac{\log 2.155 - 0.732 + 0.864 \log \Phi}{0.588}} \quad (9c)$$

RT_ R_{35}_4
$$K_4 = 10^{\frac{\log 4.427 - 0.732 + 0.864 \log \Phi}{0.588}} \quad (9d)$$

RT_ R_{35}_5
$$K_5 = 10^{\frac{\log 8.336 - 0.732 + 0.864 \log \Phi}{0.588}} \quad (9e)$$

RT_ R_{35}_6
$$K_6 = 10^{\frac{\log 16.735 - 0.732 + 0.864 \log \Phi}{0.588}} \quad (9f)$$

RT_ R_{35}_7
$$K_7 = 10^{\frac{\log 33.147 - 0.732 + 0.864 \log \Phi}{0.588}} \quad (9g)$$

RT_ R_{35}_8
$$K_8 = 10^{\frac{\log 90.804 - 0.732 + 0.864 \log \Phi}{0.588}} \quad (9h)$$

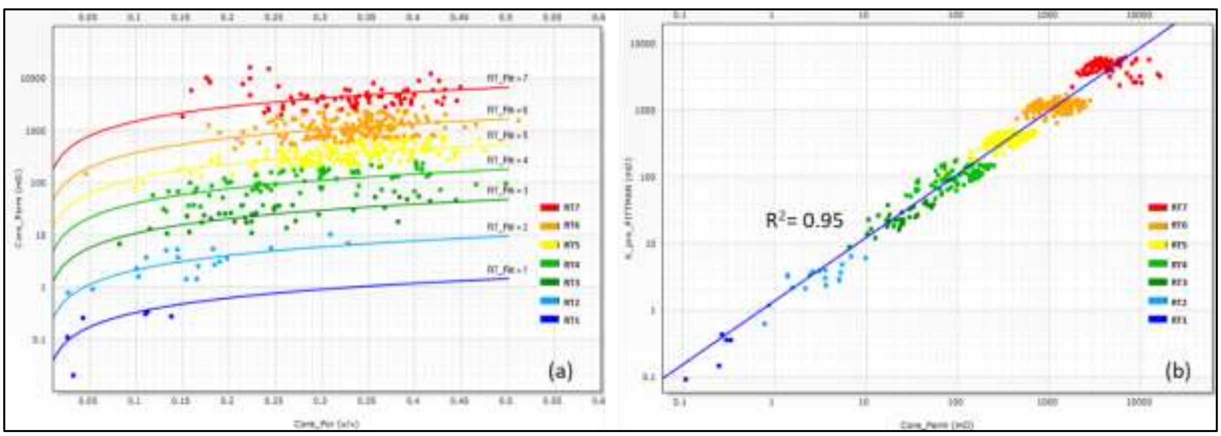

Figure 7. The results of Pittman method: (a) K_core versus PHI_core data on the background of 5 RT_pit; (b) crossplot K_pit calculated on the basis of relationship for 5 RT_pit versus K_core.

summaries the parameters for each RT_pit class. The permeability calculated (K_pre_pit) for this method uses equation 10a÷10h as appropriate. The crossplot of K_pre_pit versus K_core is shown in Figure 7b, where the correlation coefficient is $R^2 = 0.95$.

4.5. Lucia method

This is similar to the GHE method but with Lucia method we define the carbonate rock type classes by their RFN which range range from 0.5÷4. Figure 8, shows six rock types (RT_luc) distributed and corresponding with the six

Table 4. Simple statistics for 5 RTpitt.

RT_pit	Name	Start	Stop	Mean	Values	R^2
1	RT_pitt_1	0.107	0.153	0.107	1	1
2	RT_pitt_2	0.153	0.440	0.285	5	0.2935
3	RT_pitt_3	0.440	1.256	0.822	18	0.6139
4	RT_pitt_4	1.256	2.613	2.053	35	0.6094
5	RT_pitt_5	2.613	5.947	4.340	78	0.3862
6	RT_pitt_6	5.947	10.773	8.019	154	0.4474
7	RT_pitt_7	10.773	24.060	15.272	184	0.1791
8	RT_pitt_8	24.060	293.935	33.514	80	-0.3371

RT_pitt_1: $$K_1 = 10^{\frac{\log 0.127 - 0.255 + 0.523 \log \Phi}{0.565}} \quad (10a)$$

RT_pitt_2: $$K_2 = 10^{\frac{\log 0.285 - 0.255 + 0.523 \log \Phi}{0.565}} \quad (10b)$$

RT_pitt_3: $$K_3 = 10^{\frac{\log 2.053 - 0.255 + 0.523 \log \Phi}{0.565}} \quad (10c)$$

RT_pitt_4: $$K_4 = 10^{\frac{\log 4.340 - 0.255 + 0.523 \log \Phi}{0.565}} \quad (10d)$$

RT_pitt_5: $$K_5 = 10^{\frac{\log 8.019 - 0.255 + 0.523 \log \Phi}{0.565}} \quad (10e)$$

RT_pitt_6: $$K_6 = 10^{\frac{\log 0.127 - 0.255 + 0.523 \log \Phi}{0.565}} \quad (10f)$$

RT_pitt_7: $$K_7 = 10^{\frac{\log 15.272 - 0.255 + 0.523 \log \Phi}{0.565}} \quad (10g)$$

RT_pitt_8: $$K_8 = 10^{\frac{\log 33.514 - 0.255 + 0.523 \log \Phi}{0.565}} \quad (10h)$$

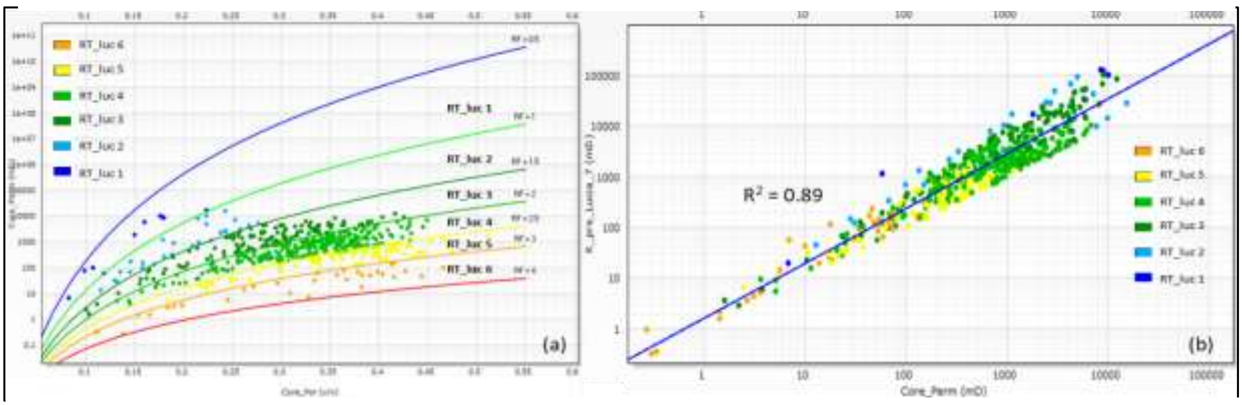

Figure 8. The results of rock type classification based on the Lucia method: (a) K_core versus PHI_core data on the background of 3 RT_luc; (b) crossplot K_luc calculated on the basis of relationship for 5 RT_luc versus K_core.

interval classes of rock fabric numbers. The rock types from RT_luc_1 to RT_luc_6 but most data falls in the range of RT_luc_2 and 3. The calculated permeability (K_pre_luc) for this method by uses equations 11a÷11f as appropriate. The crossplot of K_pre_luc versus K_core is shown in Figure 8b, where the correlation coefficient of R^2 = 0.89. Table 5 summaries some simple statistical parameters for 6 RT_luc.

On the Table 6 shows a comparison of the 5 permeability prediction models tested for the carbonate reservoirs of the NCSB. The most accurate is clearly the HFU method with R^2 = 0.97.

5. Conclusion

We tested 5 methods of rock typing using the flow unit concept. These were GHE, HFU, Winland R_{35}, Pittman and Lucia - RFN method. The samples tested came from 555 core plug data from the Miocene carbonate reservoirs, including both platform and reef. These were mainly distributed in the East of the NCSB. All of the methods showed really good correlation coefficient and higher than 89% for permeability prediction (Table 6).

In this case study, HFU method is the best method that can predict hydraulic flow unit concepts in the carbonate reservoir, therefore, this method can be applied for permeability prediction for those carbonate reservoirs.

The GHE and Lucia also give good results when classifying rock types quickly, accurately and efficiently, when applied to carbonate reservoirs with limited core data collection.

6. Recommendation

Although the different methods applied for carbonate rock typing classification from core data show good results. However, prediction of rock types in carbonates is very complex considering the various degree of heterogeneity involved and first a detailed sedimentological study needs to be done in order to understand the diagenetic imprint and its influence on the permeability. That approach was more realistic than just looking at porosity versus permeability plots and trying to derive rock types from that.

It recommends to use capillary pressure in building the initial petrophysical groups and then combined with sedimentology to have better

Table 5. Simple statistics for 3 RT_luc.

RT_luc	Name	RFN	Values	Perm R2
1	RT_luc 1	0.5	10	0.89
2	RT_luc 2	1	27	0.84
3	RT_luc 3	1.5	124	0.84
4	RT_luc 4	2	259	0.82
5	RT_luc 5	2.5	97	0.84
6	RT_luc 6	3	32	0.88

RT_luc_1 $$K_1 = 10^{(9.798+8.671\, log\Phi - log(0.5)(12.084+8.296\, log\,\Phi))} \quad (11a)$$

RT_luc_2 $$K_2 = 10^{(9.798+8.671\, log\Phi - log(1.0)(12.084+8.296\, log\,\Phi))} \quad (11b)$$

RT_luc_3 $$K_3 = 10^{(9.798+8.671\, log\Phi - log(1.5)(12.084+8.296\, log\,\Phi))} \quad (11c)$$

RT_luc_4 $$K_4 = 10^{(9.798+8.671\, log\Phi - log(2.0)(12.084+8.296\, log\,\Phi))} \quad (11d)$$

RT_luc_5 $$K_5 = 10^{(9.798+8.671\, log\Phi - log(2.5)(12.084+8.296\, log\,\Phi))} \quad (11e)$$

RT_luc_6 $$K_6 = 10^{(9.798+8.671\, log\Phi - log(3.0)(12.084+8.296\, log\,\Phi))} \quad (11f)$$

Table 6. Comparison the correlation coefficient (R^2) for 5 rock typing methods in this study.

	GHE	HFU	Winland R_{35}	Pittman R_{35}	Lucia
R^2	0.95	0.97	0.94	0.95	0.89

understanding of rock types. These rock types have been used to predict permeability and water saturation using J functions method (Leverett, 1941). This would be implemented in the future study.

Acknowledgments

This research is funded by the Vietnam National Foundation for Science and Technology Development (NAFOSTED) under grant number 105.99-2019.324. The authors gratefully acknowledge the support given by Vietnam Petroleum Institute (VPI). Techlog® software was used thanks to the university grant donation by Schlumberger to Hanoi University of Mining and Geology.

Contribution of authors

Man Quang Ha - GHE and HFU method; Hoa Minh Nguyen - introduction, methodology; Dung Viet Bui - geological setting; Hong Viet Nguyen - Winland R_{35} and pittman methods; Hoa Khac Truong - conclusion and recommendation; Ngoc Quy Pham - lucia method. All authors have read and agreed to the published version of the manuscript.

References

Abdallah, S., Sid Ali, O., & Benmalek, S. (2016). Rock type and permeability prediction using flow-zone indicator with an application to Berkine Basin (Algerian Sahara). In *SEG Technical Program Expanded Abstracts 2016* (pp. 3068-3072). Society of Exploration Geophysicists.

Amaefule, J. O., Altunbay, M., Tiab, D., Kersey, D. G., & Keelan, D. K. (1993). Enhanced reservoir description: using core and log data to identify hydraulic (flow) units and predict permeability in uncored intervals/wells. In *SPE annual technical conference and exhibition*. OnePetro. Houston, TX, USA, p. SPE-26436-MS.

Bui, V. D., Hoang, A. T., Nguyen, V. K., Ha, Q. M., Nguyen, T. T. T., Pham, T. D. H. (2018). Depositional environment and reservoir quality of Miocene sediments in the central part of the Nam Con Son basin, Southern Vietnam shelf. *Marine and Petroleum Geology*, v. 97, p. 672-689.

Corbett, P., Ellabad, Y., Mohammed, K. & Pososyaev, A. (2003). Global Hydraulic Elements - Elementary Petrophysics for Reduced Reservoir Modelling. *The 65th EAGE Conference & Exhibition,* 2-5 June 2003, Stavanger, Norway, p. cp-6-00256.

Guo, G., Diaz, M. A., Paz, F. J., Smalley, J., Waninger, E. A., (2007). Rock typing as an Effective Tool for Permeability and Water-Saturation Modeling: A Case Study in a Clastic Reservoir in the Oriente Basin. *SPE Reserv. Eval. Eng*., 10, 730-739.

Ha, Q. M., Le, N. A., & Jarzyna, J. (2021). Hydraulic flow unit classification from core data: Case study of the Z gas reservoir, Poland. *Journal of Mining and Earth Sciences. 62*(3), 29-36.

Ha, Q. M., Doan, H. H., Kieu, D. T., Bui, V. D., Nguyen, M. H., Truong, K. H., Nguyen, V. K. and Pham, Q. N. (2021b). Hydraulic Flow Unit Classification and Prediction Using Machine Learning Techniques: A Case Study from the Nam Con Son Basin, Offshore Vietnam. *Energies, 14*(22), 7714.

Haikel, S., Rosid M. S., Haidar, M. W. (2018). Study comparative rock typing methods to classify rock type carbonate reservoir Field "S" East Java. *In Journal of physics: conference series, 1120*(1), 012047. IOP Publishing.

Hartmann, D. J., & Beaumont, E. A. (1999). Treatise of Petroleum Geology/Handbook of Petroleum Geology: Exploring for Oil and Gas Traps. Chapter 9: Predicting Reservoir System Quality and Performance. *American Association Of Petroleum Geologists,* 1-154.

Kolodzie, S. (1980). Analysis of pore throat size and use of the Waxman-Smits equation to determine OOIP in Spindle Field, Colorado. *The SPE Annual Technical Conference and Exhibition,* September 1980, Dallas, Texas, USA. SPE 9382.

Leverett, M.C. (1941). Capillary Behavior in Porous Solids. *Petroleum Transactions AIME,* 142 (01), 152-169.

Lucia, F. J. (2007). Carbonate reservoir characterization: An integrated approach 2nd Edition. *Springer*. 342 p.

Matthews, S. J., Fraser, A. J., Lowe, S., Tood, S. P., Peel, F. J. (1997). Structure, stratigraphy and petroleum geology of the SE Nam Con Son basin, offshore Vietnam. *Geol. Soc. Lond. Spec. Publ*. 126, 89-106.

Palabiran, M., Sesilia, N., & Akbar, M. N. A. (2016). An analysis of rock typing methods in carbonate rocks for better carbonate reservoir characterization: a case study of Minahaki carbonate formation, Banggai Sula basin, Central Sulawesi. *41st Scientific Annual Meeting of Indonesian Associatation of Geophysicists. Lampurg.*

Pittman, E. D. (1992). Relationship porosity and permeability to various parameters derived from mercury injection capillary pressure curves for sandstone. *AAPG Bulletin*, 76, 191-198.

Rebelle, M. & Lalanne, B. (2014). Rock-typing in carbonate: a critical review of clustering methods. *Abu Dhabi International Petroleum Exhibition and Conference*, November 2014, Abu Dhabi, UAE, SPE-171759-MS.

Shenawi, S., Al-Mohammadi, H., Faquehy, M. (2009). Development of Generalized Porosity-Permeability Transforms by Hydraulic Units for Carbonate Oil Reservoirs in Saudi Arabia. *In Proceedings of the SPE/EAGE Reservoir Characterization & Simulation Conference*, 19-21 October 2009. Abu Dhabi, UAE.

Spearing, M., Allen T. & McAulay, G. (2001). Review of the Winland R_{35} method for net pay definition and its application in low permeability sands. *Special Core Analysis Symposium*, 7p.

Svirsky, D., Ryazanov, A., Pankov, M., Corbett, P. W. M., Posysoev, A. (2004). Hydraulic Flow Units Resolve Reservoir Description Challenges in a Siberian Oil Field. In *Proceedings of the SPE Asia Pacific Conference on Integrated Modelling for Asset Management*, 29-30 March 2004, Kuala Lumpur, Malaysia, p. SPE-87056-M.